X-661-76-179

PREPRINT

TMX 71178

HIGH RESOLUTION MEASUREMENTS OF THE LOW STATE OF CYG X-1

R. E. ROTHSCHILD
E. A. BOLDT
S. S. HOLT
P.J. SERLEMITSOS

AUGUST 1976

GSFC

GODDARD SPACE FLIGHT CENTER
GREENBELT, MARYLAND

(NASA-TM-X-71178) HIGH RESOLUTION MEASUREMENTS OF THE LOW STATE OF CYG X-1 (NASA) 29 p HC $4.00 CSCL 03B

N76-32086

Unclas

G3/90 03294

HIGH RESOLUTION MEASUREMENTS OF THE LOW STATE OF CYG X-1

R.E. Rothschild, E.A. Boldt, S.S. Holt, and P... Serlemitsos

NASA/Goddard Space Flight Center
Greenbelt, Maryland 20771

ABSTRACT

Cyg X-1 was observed on two occasions separated by a year (Oct. 4, 1973 and Oct. 3, 1974) by the same Goddard X-ray rocket payload. High resolution temporal and spectral data reveal that Cyg X-1 was essentially unchanged in these two observations a year apart, with bursts of millisecond duration observed in the earlier flight (Rothschild et al., 1974) observed in the second, as well. Analysis of these bursts has failed to reveal any internal temporal structure, either luminous or spectral. The shot-noise character of temporal fluctuations on timescales $\gtrsim$ 1 second can be explained by the presence of exponential pulses with a fraction of a second time constant and a rate near 8 sec^{-1}. The possible connection of these pulses with the bursts is examined.

I. INTRODUCTION

Cyg X-1 was discovered by Bowyer et al. (1965) during a rocket flight in June, 1964. Great interest in this source resulted from the UHURU observations by Oda et al. (1971) that revealed the chaotic temporal behavior of this source, including bursts of a fraction of a second duration. Rappaport et al. (1971) reported significant flaring on time-scales down to 50 ms. In a rocket flight in 1973 October, Rothschild et al. (1974) observed several bursts of 1 ms duration with high statistical certainty. This latter measurement placed the radius of the emission region at less than 10^2 km which ruled out a white dwarf as the compact object. When this compact nature of the source is combined with the mass estimates (Hutchings, 1974; Avni and Bahcall, 1975; Bolton, 1975) and the current estimates of the upper limit of the mass of a neutron star (Rhoades and Ruffini, 1974; Brecher and Caporaso, 1976), the evidence would suggest that Cyg X-1 is a black hole.

Leach and Ruffini (1973) suggested that the temporal profile of the intensity from a black hole might contain quasiperiodic structure on submillisecond timescales, and, if so, this would lead to a measurement of its intrinsic angular momentum. As a result of this suggestion and in an attempt to confirm the millisecond bursts of the previous year, an upgraded experiment with the same rocket payload of detectors viewed Cyg X-1 for three minutes on October 3, 1974 with temporal resolution a factor of two better.

The long term (> few days) behavior of Cyg X-1 may be characterized by low and high states. The low state is described by a relatively stable 2-6 keV intensity with a constant power law spectrum of photon number

index about -1.5 to -1.6 over the range 2-60 keV. The high state has a 2-6 keV intensity which is at least a factor of three higher with a steeper (and variable) spectrum (c.f. Tananbaum et al., 1972, Boldt et al., 1975, and Holt et al., 1975). Both observations reported here were made during a low state, and both at binary phase .17.

II. EXPERIMENT

Observations of Cyg X-1 were made on two occasions (Oct. 4, 1973 and Oct. 3, 1974) with a rocket-borne X-ray payload launched from White Sands Missle Range. This payload consisted of two gas proportional counters--one containing xenon-methane and the other argon-methane--giving an energy range of 1.5 to 35 keV with 128 channels of pulse height analysis. The basic temporal resolution was 320 μs on the first flight and 160 μs on the second. The time interval between the first two events in each 160μs sample was also coarsely determined on the second flight. (See Rothschild et al., 1974 for a further description of the payload). The detectors were pointed within .2° of Cyg X-1 during both flights, and the attitude control system's limit cycle during the respective exposures was ±15 arcseconds. Hence, there was no detectable modulation of the X-ray intensity due to aspect variations.

III. SPECTRAL RESULTS

Figure 1 shows the incident spectra from Cyg X-1 for the two flights as measured by both detectors. These spectra result from the analysis procedure described by Serlemitsos et al. (1975), and the best fit results are tabulated in Table I. Since the statistical uncertainties in most energy bins are quite small, the effects of an imperfect knowledge

of the detector response near the L edges of Xenon and the K edges of Argon become the dominant source of error in the inferred incident spectra.

The mean of the best fit parameters yields a power law of number index -1.55 with an upper limit of 3×10^{21} H atoms/cm^2 of cold interstellar material in the line of sight. This experiment is not sensitive to such low amounts of absorption--hence, we can only give an upper limit. This inferred upper limit of N_H is consistent with a rocket observation in 1966 October (Gorenstein et al., 1967), the OSO-7 results of 1973 January (Kwok Li and Clark, 1974) and the ANS data of 1974 November (Parsignault et al., 1976). The power law number index observed is consistent with those measured with UHURU (Tananbaum et al., 1972), OSO-7, ANS, and Ariel-5 (Sanford et al., 1976) when the source was in its low state.

The stability of the spectrum on the time scale of a minute was also investigated in the data from the second flight. The three minute exposure to Cyg X-1 was divided into three one minute observations. The three pulse height spectra derived from these exposures were identical within statistical uncertainties in the 2-20 keV range. Hence, we see no variations in the spectrum of this source either minute to minute or one year to the next with data taken at the same orbital phase (.17) when the source is in the low state.

The luminosity of this source was the same for the two flights within experimental errors. The 1.5 to 35 keV luminosity was 1.0×10^{37} ergs/sec assuming a distance of 2.5 kpc.

IV. TEMPORAL RESULTS

a) Millisecond Bursts

The discovery of eight bursts of one millisecond duration during the first flight have been reported earlier (Rothschild et al.,

1974). Five more millisecond bursts were seen in the second flight using the same criterion as before. This confirms the observations in 1973, and in a combined exposure of 230 seconds, thirteen bursts have been seen when $1.7 \pm .8$ accidentals might have been expected based on the count rate alone. This implies a duty cycle for such detectable bursting of 6×10^{-5}. We also searched for bursts on time scales from 160 μs to 5 ms, with no excess beyond that expected from Poisson fluctuations that had not been seen at one millisecond. Since burst determination depends on the local mean rate, we are less sensitive to a given intensity burst during times of enhanced activity.

The data from the second flight included additional information about the time interval between the first and second counts, if any, in each 160 μs temporal bin. These data indicated whether or not the second event occurred within 2.5 to 5.0 μs of the first or 5.0 to 50 μs of the first. The calibration of this temporal portion of the experiment was carried out using radioactive sources as random pulse generators to induce various rates in the payload and then directly noting the rates in the various temporal ranges. Table II shows the distribution of the time intervals for the five bursts observed in the second flight along with expectations of this distribution for random events at the observed intensities.

The time interval data from burst #3, with 18 counts in 1.28 ms, is in marked disagreement with the predictions based on random rates. This burst (the hardest (spectrally), as well as most intense observed in the two flights), showed an excess of counts on the 2.5 - 5 μs scale

and a deficiency of counts on the 5-50 μs scale. The remaining four, on the other hand, indicate that the internal structure of the bursts is random within the coarse statistical uncertainties. As a result, the most intense burst (#3) has not been included in any of the subsequent analyses of bursts in general.

One of the purposes of this experiment was to investigate the possible substructure of these bursts. Such substructure could yield a value for the intrinsic angular momentum of the collapsed object (Leach and Ruffini, 1973). Scrutinizing individual bursts for structure is essentially useless due to the statistical uncertainties associated with so few counts. Instead a composite burst profile was created by aligning the intensity centroid of each burst--this being the only temporal reference for this aperiodic phenomenon. The rate data were binned as finely as possible and the result for four of the five bursts seen in the second flight is shown in Figure 2a. No significant substructure is obvious on this 160 μs/bin scale. The dotted line is the non-burst intensity (calculated locally over the 3.5 ms displayed) plus a one millisecond rectangular pulse aligned with the centroid containing the same number of counts as the four bursts. The composite burst for the twelve events in both flights is displayed on a 320 μs/bin scale in Figure 2b. No significant internal structure can be seen. Hence, on both flights the measurements are consistent with a constant intensity throughout a burst with a duration of one millisecond.

Inferring the burst incident spectrum from the 53 pulse height values sampled in the thirteen bursts is plagued by statistical uncertainties,

so that, the mean observed energy for each burst has been calculated along with its formal uncertainty. This parameter has also been calculated for the overall emission. The result is shown in Table III. The anamolous burst #3 mentioned above has by far the greatest mean energy and uncertainty. Since this event is apparently anomalous, it is not included in the following analysis. The mean observed burst energy is 2 1/2 standard deviations less than that of the overall emission, while the mean observed energy of the eight first flight bursts are consistent with the four second flight bursts. The anamolous burst is harder than the overall emission, but in fact is only 1.9 standard deviations above the mean observed burst energy. The distribution of mean observed energies about their mean was calculated in order to determine if (within statistics) the twelve bursts came from the same spectral population. The χ^2 was not acceptable, but this was due entirely to burst #8 with its small uncertainty. Hence, our data are consistent with a situation where most of the bursts display a common spectral and temporal character.

Finally, the mean observed burst energy versus burst intensity is shown in Figure 3. The highest point marked with the asterisk is the anomalous burst #3 mentioned above. No drastic variation in mean energy is seen with intensity, even though a better fit is obtained if one considers a slow increase in energy with intensity as opposed to a constant value.

b) Shot Noise

The fluctuations in intensity of Cyg X-1 on time scales of tenths to tens of seconds are not Poisson in nature. It has been shown (Terrell, 1972; Boldt <u>et al</u>., 1975 and references therein) that the major

features of the intensity variations can be described as the superposition of randomly occuring, overlapping, exponentially shaped pulses (i.e. shot noise).

The mean shot pulse wave form can be determined through the use of the autocorrelation function (see e.g. Papoulous, 1965; Brigham, 1974; or Jenkins and Watts, 1969; Weisskopf, 1975). If the single pulse shape as a function of time, t, is described by h(t) for $t \geq 0$ and zero elsewhere, then the autocorrelation function, $\rho(\tau)$., is given by

$$\rho(\tau) = \frac{\int_0^{\infty} h(t) \quad h(t + \tau) \quad dt}{\int_0^{\infty} h^2(t) \quad dt}$$

where τ is the lag parameter. In the case of exponential shaped pulses ($h(t) = Ae^{-t/\tau_o}$), the autocorrelation function is also an exponential ($\rho(\tau) = e^{-\tau/\tau_o}$).

The data from the two flights were divided into 20 second intervals, and $\rho(\tau)$ was calculated in the energy ranges 2.5 - 5.1 keV, 5.1 - 12 keV, 12 - 40 keV, and 2.0 - 40 keV, and is shown in Figure 4. The resulting autocorrelation functions can be described by an exponential with a fraction of a second decay time, where the lag parameter is quantized in 20.48 ms bins. The variations from $\rho(\tau) = 0$ for $\tau > 1$ second are due to aliasing by the shot noise character of the data, finite statistics, and a finite exposure, and are NOT necessarily indicative of additional, longer period phenomena. This conclusion is based upon computer simulations of the shot noise process. The same analysis was applied to the Cyg X-3 exposure during the first flight, which had a comparable count rate, and $\rho(\tau)$ was consistent with random data. Also, no oscillatory behavior was seen for $\tau > 1$ second.

The resultant autocorrelation functions were fit to an exponential (with amplitude and decay time as free parameters) by a least squares method. The decay time along with the mean rate for each exposure is displayed in Table IV. The fitted values of the decay time vary from .24 s to 1.40 s throughout our exposures, while the mean counting rates vary significantly less. This indicates that the rate of shot pulses must also vary--perhaps as much as a factor of four on time scales of tens of seconds. Halfway through the second flight the decay time abruptly increased in all energy ranges, and this situation persisted for at least a minute. An examination of correlations between the 2.1 - 5.1 keV data and the 5.1 - 12.0 keV data revealed that they were correlated, and that any time delay between the two regimes had to be less than 10 ms, if indeed any delay existed at all.

In order to estimate the shot pulse rate the variance for both flights was calculated as a function of integration time. In the case of a source of random intensity variations, the variance is independent of integration time, and equals the mean rate. It was indicated by Boldt et al. (1975) that in the case of a source dominated by shot-noise intensity fluctuations the variance is independent of integration time only for times long compared with the individual shot pulses. In this case the variance per unit bin width is $(1 + f^2 \mu/\lambda)\mu$ where μ is the mean rate, λ is the shot pulse rate, and f is the fraction of the overall rate due to shot noise. Unless very long exposures are used, the uncertainty in the variance for long integration times is considerable. Hence, a mean value of λ can be found only for the entire second flight. The

plot of variance per unit bin width vs. bin width is shown in Figure 5 for the second flight. In this case $\lambda = 7.9 \pm .5$ sec^{-1} assuming that the intensity was entirely due to shot noise.

Weisskopf, Kahn and Sutherland (1975) have studied the UHURU observations of Cyg X-1 and find that the shot pulses produce an exponentially shaped autocorrelation function with decay times in the range $.5 \pm .1$ seconds. If they assume the flux to be entirely shot pulse generated, they arrive at a pulse rate in the range 9 - 15 pulses/second (Weisskopf, 1976) in agreement with our result.

A Monte Carlo simulation of the shot noise process was performed using a single shot pulse shape. The major features of the Cyg X-1 intensity variations on the .1 to 50 second time scale were replicated. However, the fraction-of-a-second enhancements (e.g. see fig. 1, Rothschild et al. (1974)) seen in both flights were not evident. This could be evidence for a more complicated shot noise process with varying pulse amplitudes and/or decay times, or it could imply that these particular enhancements are not associated with the shot pulses.

It should be pointed out that the shot pulse rate, decay time, the fraction of the intensity due to shot noise, and the intensity of a single shot pulse cannot each be unambiguously determined at this time. The decay time is measured by fitting the autocorrelation function. The shot pulse rate λ is dependent on the shot noise intensity. This, however, cannot unambiguously be separated from the overall intensity. The intensity of a single shot pulse can be determined from the variance of the portion of the intensity due to the shot noise, which again is dependent on the

fraction of the overall intensity due to shot noise. Thus, we can deduce a consistent (but not unique) characterization of the processes involved in the X-ray emission from Cyg X-1.

c) Fourier Analysis

Since the discovery of fast temporal variations in this source (Oda et al., 1971), much interest has been shown in searching for a pulsed component to the intensity. This would be compelling evidence of a neutron star as the compact object. Several periods have been seen in the fourier analysis of short time intervals (see Boldt et al., 1975 and references therein), but none seem to be persistent. This is just the behavior that a shot-noise model would predict.

The three minute exposure to Cyg X-1 of the second flight was divided into 10 second intervals and searched for periodicities using a standard FFT program. In all intervals the majority of the power was in frequencies less than 10 Hz as expected for shot noise fluctuations with $\tau \gtrsim 0.1$ s. No one frequency was present at the less than 10^{-4} probability level in all intervals, and no interval was free of this low frequency power. When the same techniques were applied to the Cyg X-3 exposure, no frequencies less than 10 Hz had a probability less than 10^{-4}. Thus we conclude that the low frequency power seen in the Cyg X-1 data is indeed due to fluctuations at this source and not due to rocket motion or aliasing by the finite exposure. These results are similar to the dynamic spectrum analysis of Oda et al. (1975) where the power was seen to concentrate below a few Hz.

V. DISCUSSION

We have observed Cyg X-1 in its low state on two occasions, both at the same phase of the binary system, and have detailed spectral and temporal information. First, the spectrum from 1.5 to 35 keV is a featureless power law of number index -1.55 with low energy absorption less than 3×10^{21} H atoms/cm^2 in the line of sight. This spectral signature is indicative of the low state, and has been seen at various times since 1966. The Pringle and Rees (1972) spectral form expected for accretion onto a compact object from a uniform ($\lambda = \mu = 0$) disk, where "free-free" emission dominates is a power law with a number index of -1.5, in good agreement with observations of the low state. Shapiro, Lightman and Eardley (1975) have modelled the accretion disk of Cyg X-1, and also predict a power law spectrum in this energy range. Using our measured value of the index and their analytic form, we find

$$.51 = \frac{kT_e}{m_e c^2} \cdot N_{scat}$$

where $\frac{kT_e}{m_e c^2}$ is the high energy cutoff energy in units of the electron rest mass and N_{scat} is the number of scatterings experienced by a photon before emerging from the cloud. A balloon observation made in late August of 1967 (Haymes et al., 1968) found that an exponential with $kT_e \approx 95$ keV fit the data as well as two power laws. Nine days later Meekins et al. (1969) observed Cyg X-1 from 1.5 - 12 keV and found its spectrum to be a power law of number index -1.5. Assuming it was in the low state nine days earlier, $kT_e \approx 95$ keV should be indicative of the low state cutoff energy. Matteson et al. (1976) report a low state cutoff energy of $kT \approx 85$ keV in 1969 when rocket observations

also imply the low state. Inserting kT_e = 90 keV into the above equation yields N_{scat} = 2.8. This implies that the optical depth for Thomson scattering is greater than one. Hence it is not surprising that the observed spectrum is featureless.

Ryter, Cesarsky and Audouze (1975) and Gorenstein (1975) have derived a relationship between interstellar reddening and X-ray absorption, and Margon, Bowyer, and Stone (1973) measured the extinction in the line of sight to Cyg X-1. Combining these two results gives a value of $(7.5 \pm 1.8) \times 10^{21}$ H atoms cm^{-2} for the interstellar absorption. This is a factor of two greater than our upper limit, but still indicates a minimum of circumstellar absorption.

Cyg X-1 exhibits variability on several time scales ranging from millisecond pulses to high and low states lasting for a hundred days or more (Holt et al., 1976). Recently, Canizares (1976) has postulated that the giant X-ray bursts seen from 3U1820-30 can be the result of shorter bursts of X-rays emitted inside an optically thick hot cloud and then reverberating within the cloud, and that this may be the case for Cyg X-1, as well. The millisecond pulses, only occassionally seen, might be the embedded pulses and the shot noise pulses are the result of the scattering in the cloud. As discussed above the optical depth for Thomson scattering is greater than one, implying the presence of a hot cloud. The millisecond pulses would not be expected to be observable through an optically thick cloud but the shot noise reverberations would. The fact that the only observed instance of bursts bunched together occurred during the peak of a period of enhanced intensity, might be explained

by a local thinning of the cloud due to the increased X-ray flux. Taking the three bursts observed during the peak of the enhancement (see Fig. 2, Rothschild et al., 1974) as representative of the basic millisecond pulse rate, an order of magnitude estimate of the millisecond pulse rate (100 pulses/sec) is about 10 times the derived shot noise pulse rate ($\sim$ 8/sec). This would imply that the driving millisecond pulses are not 100% efficient in creating observable shot pulses. On the other hand, the enhanced intensity could have been caused by a period of enhanced millisecond pulse rate, thus causing the estimate of the millisecond pulse rate to be larger than nominal.

As noted above the mean observed energy of the millisecond bursts is 2 1/2 standard deviations less than that of the overall emission if the one anomalous burst (#3) is excluded from the sample. This is consistent with Canizares' model where the driver pulse is softer than the reverberation or shot pulse. This, then, would suggest a softer component embedded in the accretion cloud. Garmire and Ryter (1975) and Gorenstein (1975) suggested that the anomalously low measured X-ray absorption noted above during the low state might be explained by the presence of an additional soft X-ray component at the source.

Finally, we can estimate the energy of the bursts and the shot noise pulses observed in the two flights. The data indicate that a burst contains 10^{35} ergs and an individual shot pulse contains f x 10^{36} ergs, where f is the fraction of the overall emission due to shot noise.

There remains the explanation of the source of the millisecond bursts. Sunyaev (1973) has suggested that the turbulence in the accretion

disk can lead to hot matter being convected out from the inner portions of the cloud, and that these hot spots can exist for times on the order of the orbit time. The duration of these events then depends upon the angular momentum of the collapsed object. Then, the minimum period for a non-rotating blackhole is $\sim .5\ (M/M_o)$ms, and for a maximally rotating blackhole is $\sim .06\ (M/M_o)$ms, where M is the mass of the blackhole (Novakov and Thorne, 1972). If the millisecond bursts observed are a result of this process, the nonrotating case would predict a mass on the order of 2 M_o whereas the maximally rotating case would predict a mass on the order of 17 M_o. The derived mass of Cyg X-1 is in the range 8-15 M_o (Hutchings, 1974; and Avni and Bahcall, 1975). Thus, the model of Sunyaev would indicate that the collapsed object is rotating and that the Schwarzschild metric is not applicable. It also should be noted that the burst intensities dominate the overall emission when present, and are not in the nature of a small perturbation.

VI. ACKNOWLEDGEMENTS

It is a pleasure to acknowledge the splendid payload preparation work of C. Glasser, F. Birsa, M. Ziegler, and E. Karageorge. Our thanks also to the Goddard Space Flight Center sounding rocket division and the launch crew at White Sands Missle Range for their fine work and cooperation.

FIGURE CAPTIONS

Figure 1 — Inferred incident spectrum of Cyg X-1 observed on both flights. The solid circles represent the spectrum seen by the xenon detector and the open circles represent the spectrum seen by the argon detector.

Figure 2a — Centroid-aligned mean burst profile for the Oct. 3, 1974 observation of Cyg X-1. The temporal bins are 160 μs wide and the data are from four superimposed bursts. The dotted line represents the expected burst profile for a 1 ms wide rectangular pulse containing the same number of counts as the four bursts.

Figure 2b — Centroid-aligned mean burst profile for the 8 bursts seen in Oct., 1973 and the 4 bursts seen in Oct., 1974. The temporal bins are 320 μs wide. The dotted line represents the expected burst profile for a 1 ms wide rectangular pulse containing the same number of counts as the twelve bursts.

Figure 3 — Variation of burst mean energy with burst intensity. The asterisk denotes the anomalous burst (#3) mentioned in the text.

Figure 4 — The autocorrelation functions, $\rho(\tau)$, versus lag parameter, τ, for 20 seconds of exposure during the Oct., 1973 flight, as a function of energy. The energy ranges are 2-35 keV at the top, 2-5 keV second from the top, 5-10 keV second from the bottom, and 10-35 keV at the bottom.

Figure 5 — Variance per unit bin width versus bin width for the Oct., 1974 flight. The dotted line shows the mean count rate of Cyg X-1.

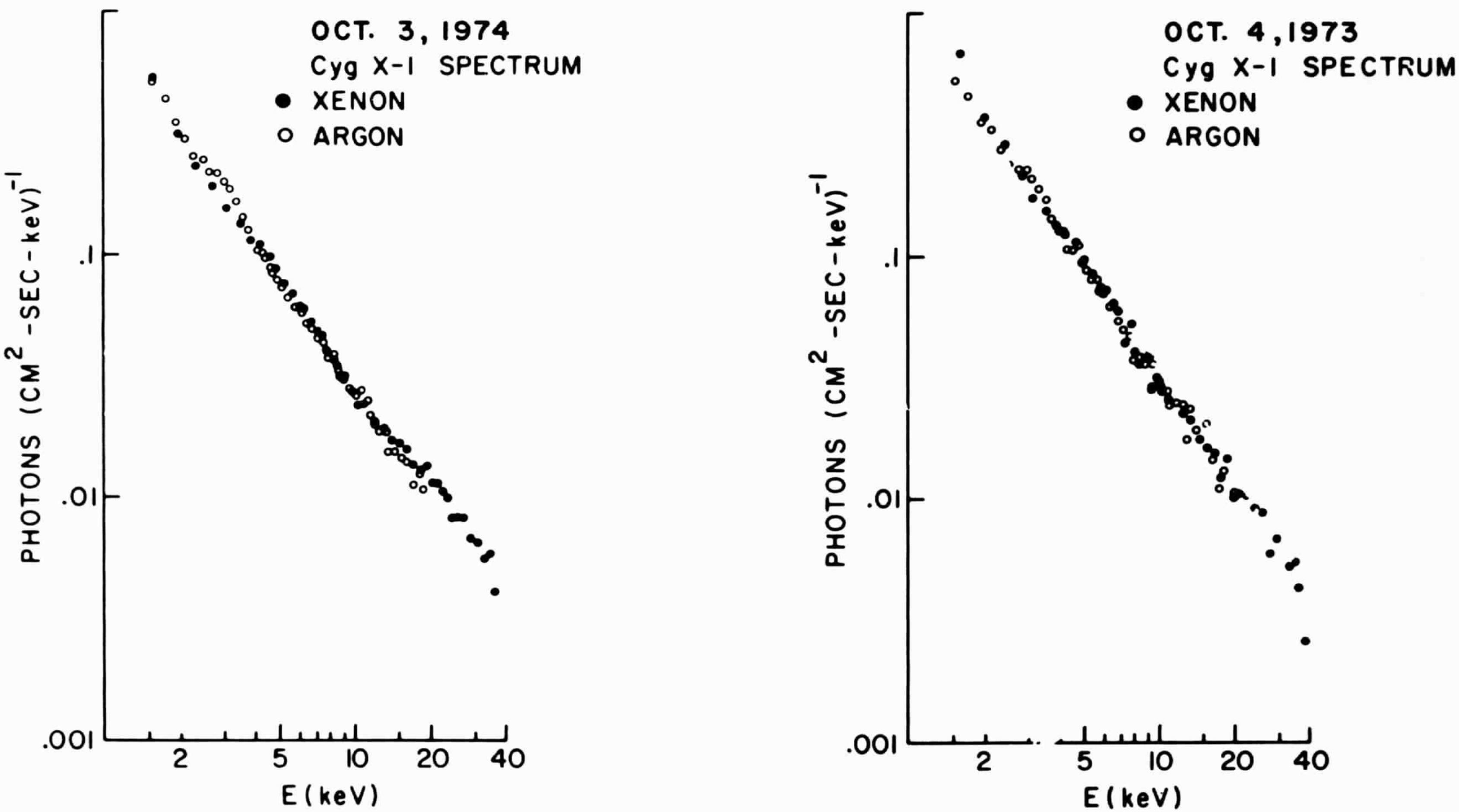
OCT. 3, 1974
Cyg X-1 SPECTRUM
XENON
ARGON
PHOTONS (CM^2-SEC-keV)$^{-1}$
.1
.01
.001
2
5
10
20
40
E (keV)
OCT. 4, 1973
Cyg X-1 SPECTRUM
XENON
ARGON
PHOTONS (CM^2-SEC-keV)$^{-1}$
.1
.01
.001
2
5
10
20
40
E (keV)

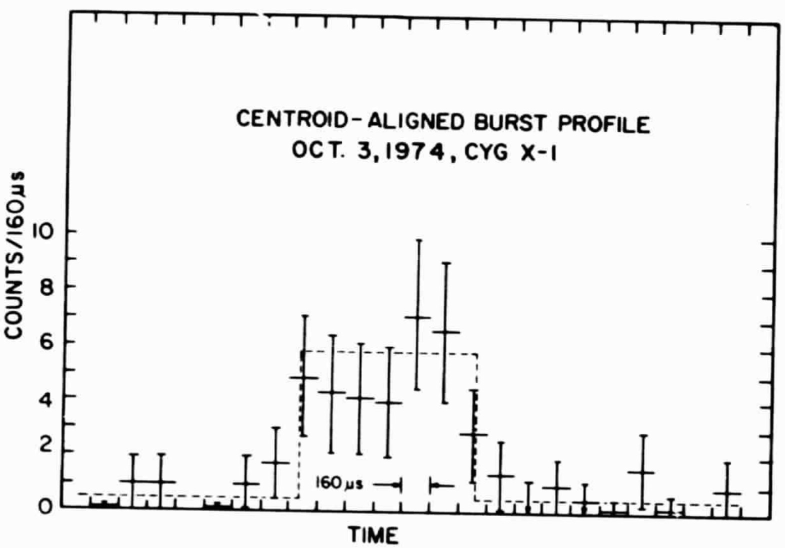
CENTROID-ALIGNED BURST PROFILE
OCT. 3, 1974, CYG X-1
COUNTS/160 μs
0
2
4
6
8
10
160 μs
TIME

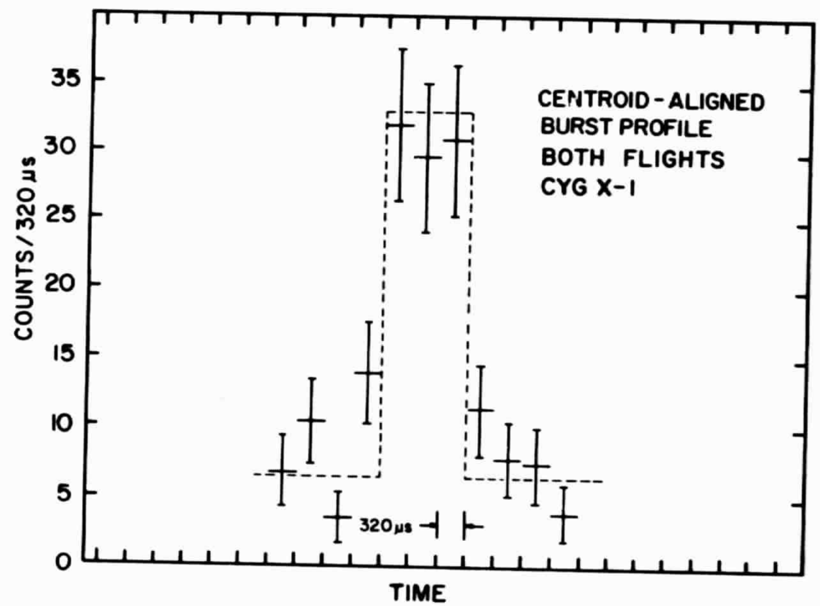
CENTROID-ALIGNED
BURST PROFILE
BOTH FLIGHTS
CYG X-1
COUNTS/320 μs
0
5
10
15
20
25
30
35
320 μs
TIME

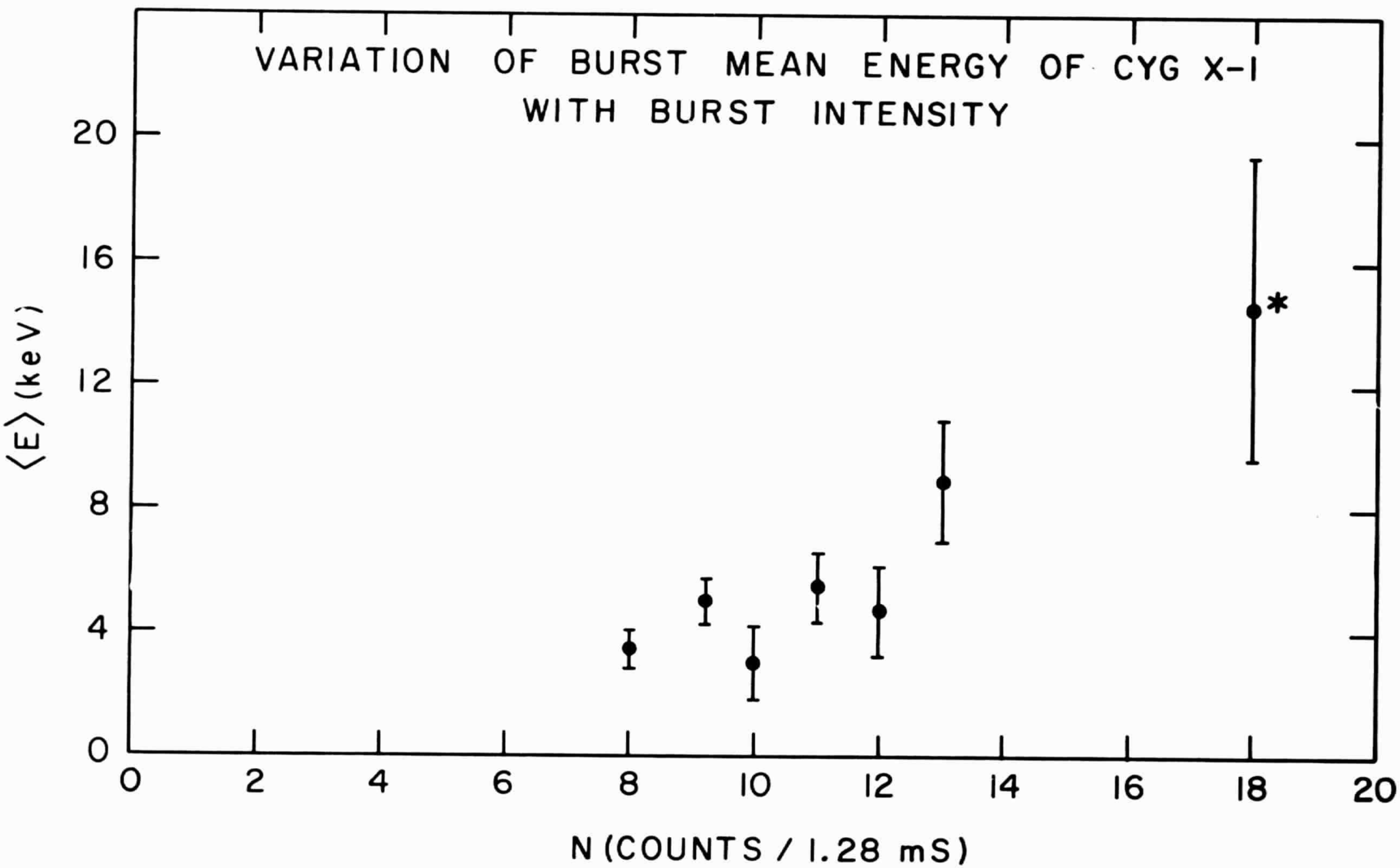
VARIATION OF BURST MEAN ENERGY OF CYG X-1
WITH BURST INTENSITY
⟨E⟩ (keV)
0
4
8
12
16
20
0
2
4
6
8
10
12
14
16
18
20
N (COUNTS / 1.28 mS)
*

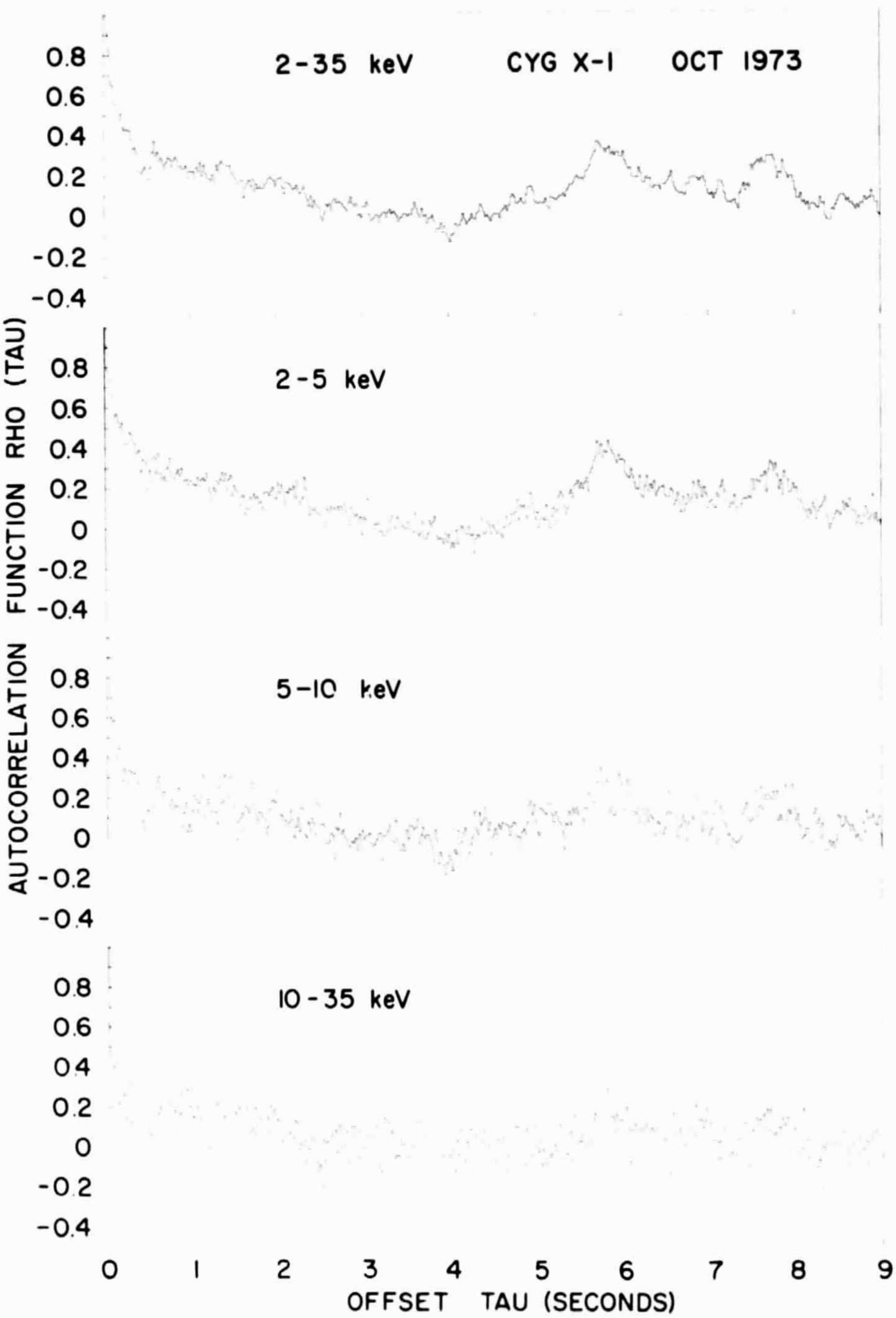

2-35 keV
CYG X-1 OCT 1973
2-5 keV
5-10 keV
10-35 keV
AUTOCORRELATION FUNCTION RHO (TAU)
0.8
0.6
0.4
0.2
0
-0.2
-0.4
0 1 2 3 4 5 6 7 8 9
OFFSET TAU (SECONDS)

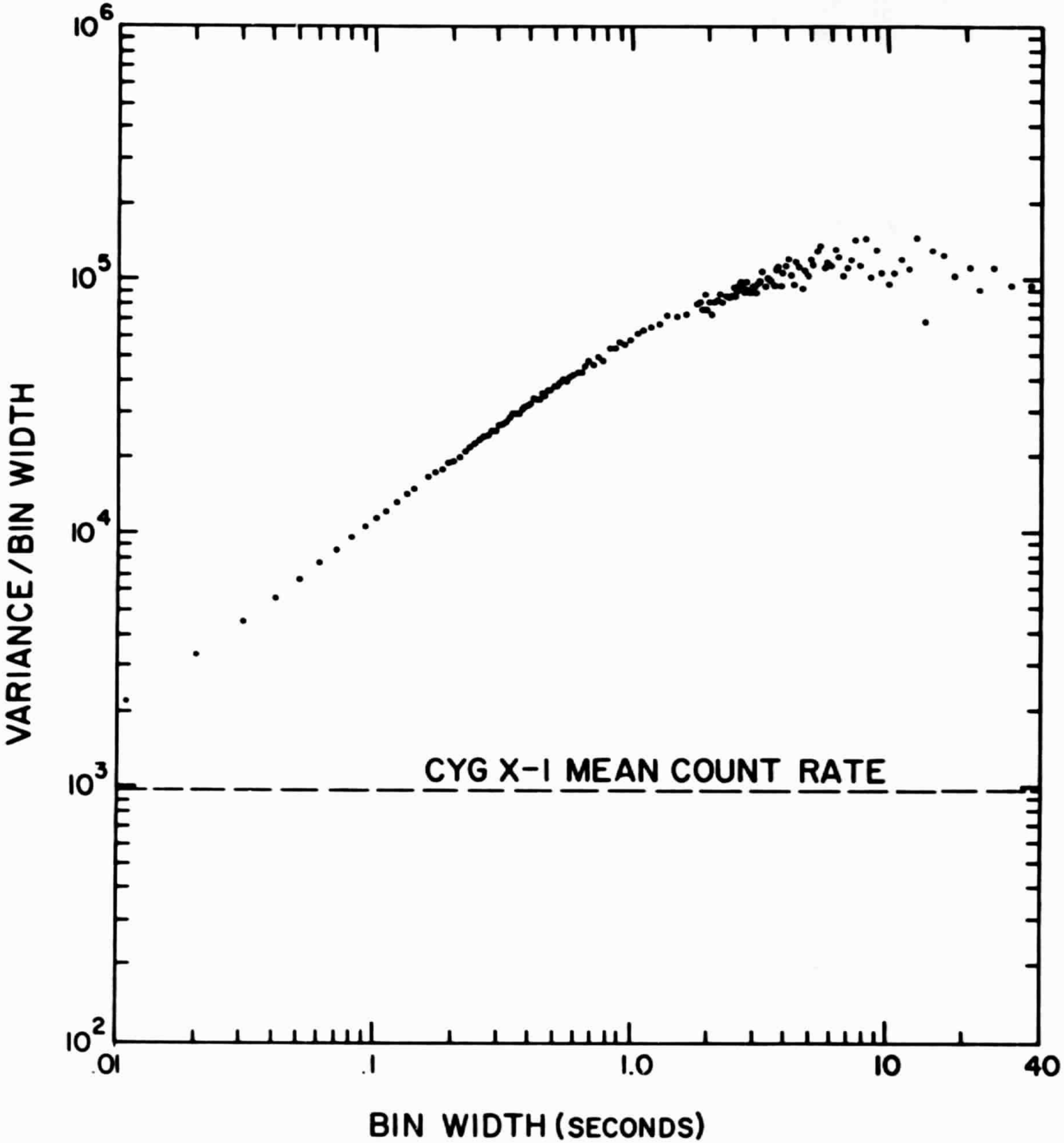

10^6
10^5
10^4
10^3
10^2
VARIANCE/BIN WIDTH
CYG X-1 MEAN COUNT RATE
.01
.1
1.0
10
40
BIN WIDTH (SECONDS)

TABLE I

BEST FIT SPECTRAL PARAMETERS*

FLIGHT	DETECTOR	INDEX	E_a(keV)	χ^2	f
Oct 1973	Xe	-1.57	$\leq$ .76	41	13
Oct 1973	Ar	-1.58	$\leq$ .86	36	11
Oct 1974	Xe	-1.47	$\leq$ .77	176	13
Oct 1974	Ar	-1.60	$\leq$ .85	66	11
Average		-1.55	$\leq$ .81		

*assumed spectral form is $\phi(E) = e^{\mathrm{INDEX}}\, e^{-(E_a/E)^{8/3}}$ and χ^2 is the total chi-squared value for the fit using f degrees of freedom for a single detector.

TABLE II

DISTRIBUTION OF TIME INTERVALS BETWEEN FIRST AND SECOND COUNTS

IN 160 μs FOR OCT 1974 FLIGHT

BURST #	COUNTS/1.28ms	OBSERVED 2.5-5.0μs	OBSERVED 5.0-50μs	EXPECTED 2.5-5.0μs	EXPECTED 5.0-50μs
1	8	0	1	.07	1.5
2	9	0	1	.09	1.9
3	18	3	3	.37	6.0
4	9	0	2	.09	1.9
5	11	0	2	.10	2.6

TABLE III

MEAN OBSERVED ENERGY FOR EACH BURST

OCT 1974	COUNTS/1.28ms	[E](keV)	σ([E])(keV)
BURST # 1	8	3.4	.6
# 2	9	5.2	1.2
# 3	18	14.5	4.9
# 4	9	3.6	1.0
# 5	11	4.7	1.0
OCT 1973			
BURST # 6	11	6.2	1.9
# 7	9	5.1	1.6
# 8	10	2.4	.4
# 9	10	4.2	1.6
#10	13	4.7	1.5
#11	11	7.7	3.3
#12	12	8.9	2.0
#13	9	5.6	1.5

TABLE IV

MEAN INTENSITY (μ) IN COUNTS/SEC AND SHOT NOISE DECAY TIME (τ_o) IN SECONDS FOR 10 SECOND EXPOSURES TO CYG X-1

	2.1 - 40 keV		2.1 - 5.1 keV		5.1 - 12 keV		12 - 40 keV	
OCT 1974	μ	τ_o	μ	τ_o	μ	τ_o	μ	τ_o
INTERVAL # 1	838	$.35\pm.02$	403	$.42\pm.03$	315	$.31\pm.02$	120	$.21\pm.04$
# 2	1026	$.31\pm.02$	493	$.18\pm.03$	390	$.36\pm.04$	142	$.65\pm.37$
# 3	1045	$.24\pm.01$	505	$.30\pm.03$	396	$.22\pm.02$	144	$.10\pm.05$
# 4	1065	$.25\pm.01$	506	$.31\pm.02$	409	$.24\pm.02$	150	$.15\pm.02$
# 5	845	$1.40\pm.11$	412	$1.48\pm.19$	320	$1.13\pm.23$	112	*
# 6	994	$.69\pm.05$	489	$.88\pm.07$	371	$.53\pm.05$	134	$.63\pm.11$
# 7	987	$.53\pm.02$	483	$.55\pm.02$	374	$.53\pm.02$	130	$.45\pm.04$
# 8	958	$.56\pm.02$	466	$.82\pm.06$	364	$.36\pm.02$	128	$.82\pm.34$
OCT 1973								
INTERVAL # 1	1340	$.23\pm.02$	695	.30	479	$.18\pm.04$	166	$.10\pm.06$
# 2	1207	$.34\pm.02$	610	.33	443	$.34\pm.04$	154	$.54\pm.18$

*Unable To Fit Autocorrelation Function

REFERENCES

Avni, Y. and Bahcall, J. N. 1975, Ap. J., 197, 675.

Boldt, E., Holt, S., Rothschild, R. and Serlemitsos, P. 1975, "International Conference on X-Rays in Space", 1, 69.

Bolton, C. T. 1975, Ap. J., 200, 269.

Bowyer, S., Byram, E. T., Chubb, T. A., and Friedman, H. 1965, Science, 147, 394.

Brecher, K. and Caporaso, G. 1976, Nature, 259, 377.

Brigham, E. O. 1974, The Fast Fourier Transform, (Englewood Cliffs, N.J.: Prentice-Hall).

Canizares, C. 1976, (MIT preprint).

Garmire, G. P. and Ryter, C. E. 1975, Astrophysical Letters, 16, 121.

Gorenstein, P., Giacconi, R., and Gursky, H. 1967, Ap. J. (Letters), 150, L85.

Gorenstein, P. 1975, Ap. J., 198, 95.

Haymes, R. C., Ellis, D. V., Fishman, G. J., Glenn, S. W., and Kurfess, J. D. 1968, Ap. J. (Letters), 151, L125.

Holt, S. S., Boldt, E. A., Kaluzienski, L. J., and Serlemitsos, P. J. 1975, Nature, 256, 108.

Holt, S. S., Boldt, E. A., Serlemitsos, P. J., and Kaluzienski, L. J. 1976, Ap. J. (Letters), 203, L63.

Hutchings, J. B. 1974, Ap. J. (Letters), 193, L61.

Jenkins, G. M. and Watts, D. G. 1969, Spectral Analysis and Its Applications, (San Francisco: Holden-Day).

Kwok Li, F. and Clark, G. W. 1974, Ap. J. (Letters), 191, L27.

Leach, R. and Ruffini, R. 1973, Ap. J. (Letters), 180, L15.

Margon, B., Bowyer, S. and Stone, R. P. S. 1973, Ap. J. (Letters), 185, L113.

Matteson, J. L., Mushotzky, R. F., Paciesas, W. S., and Laros, J. G. 1976, "Symposium on X-Ray Binaries", NASA SP-389, 1976.

Meekins, J. F., Henry, R. C., Fritz, G., Friedman, H., and Bryan, E. T. 1969, Ap. J., 157, 197.

Novakov, I. D. and Thorne, K. S. 1972, Black Holes, C. DeWitt and B. S. DeWitt eds. New York: Gordon and Breach), Chapter 6.

Oda, M., Gorenstein, P., Gursky, H., Kellogg, E., Schreier, E., Tananbaum, H., and Giacconi, R. 1971, Ap. J. (Letters), 166, L1.

Oda, M. Dai, K., Ogawara, Y., Takagishi, K., and Wada, M. 1975, "Symposium on Fast Transients in X- and Gamma-rays", preprint.

Papoulis, A. 1965, Random Variables, and Stochastic Processes, (New York: McGraw-Hill).

Parsignault, D. R., Grindlay, J. E., Schnopper, H., Schreier, E. J., and Gursky, H. 1976, "Symposium on X-Ray Binaries", NASA SP-389.

Pringle, J. S. and Rees, M. J. 1972, Astron. and Astrophys., 21, 1.

Rappaport, S., Doxey, R., and Zaumen, W. 1971, Ap. J. (Letters), 168, L43.

Rhoades, C. E., and Ruffini, R. 1974, Phys. Rev. Lett., 32, 324.

Rothschild, R. E., Boldt, E. A., Holt, S. S., and Serlemitsos, P. J. 1974, Ap. J. (Letters), 189, L13.

Ryter, C., Cesarsky, C. and Audouze, J. 1975, Ap. J., 198, 103.

Sanford, P. W., Ives, J. C., Bell Burnell, S. J., Mason, K. O., and Murdin, P. 1975, Nature, 256, 109.

Serlemitsos, P. J., Boldt, E. A., Holt, S. S., Rothschild, R. E., and Saba, J. L. R. 1975, Ap. J. (Letters), 201, L9.

Shapiro, S. L., Lightman, A. P., and Eardley, D. M. 1975, Ap. J. (in press).

Sunyaev, R. A. 1973, Soviet Astron.-AJ, 16, 941.

Tananbaum, H., Gurskey, H., Kellogg, E., and Giacconi, R. 1972, Ap. J. (Letters), 177, L5.

Terrell, N. J. 1972, Ap. J. (Letters), 174, L35.

Weisskopf, M. C., Kahn, S. M., and Sutherland, P. G. 1975, Ap. J. (Letters), 199, L147.

Weisskopf, M. C. 1976, private communication.